Marko Mumović, Nikola Šibalić, Darko Bajić, Milan Vukčević*

NUMERICAL ANALYSIS OF WELDING SEQUENCE INFLUENCING THE QUALITY OF AN AA6060-T4 ALLOY LAP JOINT

NUMERIČKA ANALIZA UTICAJA SEKVENCE ZAVARIVANJA NA KVALITET PREKLOPNOG SPOJA LEGURE AA6060-T4

Originalni naučni rad / Original scientific paper
UDK /UDC:
Rad primljen / Paper received: 28.6.2021

Adresa autora / Author's address:
University of Montenegro, Faculty of Mechanical Engineering, Podgorica, Montenegro, darko@ucg.ac.me

Keywords
- arc welding simulation
- gas metal arc welding (GMAW)
- finite element modelling
- lap joint
- aluminium alloy
- welding sequence

Abstract

The application of different strategies for performing welding sequences can affect the quality of the welded joint. The goal of different strategies is the priority in achieving minimal degrees of distortion of welded testpieces. These strategies are especially important for long seam welded joints. In this paper, the segmentation order is optimised using finite element software (FEM) for the AA6060-T4 lap joint of the GMAW welded plates. Input parameters of the numerical simulation are presented in detail. The effects of temperature and residual stress distributions as direct causes of distortion are analysed. Results of these simulations show that adequate sequence selection can reduce welding distortion values by as much as 30 %.

Ključne reči
- simulacija elektrolučnog zavarivanja
- elektrolučno zavarivanje u zaštiti gasom (GMAW)
- modeliranje konačnim elementima
- preklopni spoj
- legura aluminijuma
- sekvenca zavarivanja

Izvod

Primena različitih strategija za izvođenje sekvenci zavarivanja može u velikoj mjeri uticati na kvalitet zavarenog spoja. Cilj različitih strategija je prvenstveno formiranje kvalitetnog zavarenog spoja sa minimalnim stepenom distorzije zavarenih radnih komada. Ove strategije su posebno važne za duge zavarene spojeve. Izvršena je optimizacija redosleda segmentiranja upotrebom softvera na bazi konačnih elemenata (FEM) za preklopni spoj ploča od AA6060-T4, zavarenih GMAW postupkom. Ulazni parametri numeričke simulacije su detaljno predstavljeni. Uticaji raspodele temperature i zaostalih napona su analizirani kao direktni uzroci distorzije. Rezultati simulacija pokazuju da adekvatan odabir sekvence može smanjiti vrednosti distorzije za čak 30 %.

INTRODUCTION

Welding is defined as localized adhesion of metals or non-metals caused by either heating the material to the appropriate temperature with or without the effect of pressure, or only the effect of pressure, with or without the use of additional material /1/. Welding technologies are the most commonly used and most important joining technologies in the industry. Numerous welding technologies are based on the electric arc. Today, over 90 welding processes are in use /2/, of which arc welding processes are by far the most presented. They are considered main joining processes and are widely used in all industries due to their efficiency and economical benefits /3/. When designing new products, engineers tend to find the best balance between strength and stiffness of parts, while keeping costs as low as possible. Due to these requirements, aluminium alloys stand out in many applications and are materials of choice in many engineering applications. Despite the development of arc welding processes, weld-induced stresses and distortions remain to be a huge obstacle in the manufacture of light structures. This is especially pronounced in thin sheet materials. Since aluminium heats up locally very fast, the distribution of internal temperature is very uneven. This, combined with aluminium high heat conductance and lower strength at elevated temperatures leads to relatively high residual stresses and distortions, which can result in instability of mechanical characteristics and thus limiting their application.

These unfavourable welding consequences can be diminished by an adequate choice of welding process parameters and proper welding setup. Arc welding is a complex process, influenced by many parameters including electrical, kinematic, geometric, and many more, whose combination can greatly influence welding distortion and residual stresses. Conduction of real-world experiments to find optimal parameters is expensive and time-consuming, so this task can be solved by using welding simulation software, /4/.

One of the main methods of improving joint quality, primarily used in long welds is splitting the procedure into segments, /5/. Welding of these segments by a certain order makes a sequence. By optimisation of performance order of these segments, negative attributes of the process can be greatly affected. This is also affected by choice of welding process, as its nature reflects on the weld quality.

This paper analyses several sequences of segments performance order, by using leading CAE software Simufact Welding, based on the finite element method (FEM).

The development of numerical simulation software has given researchers a powerful tool for analysing weld properties, which were previously limited to physical measurements. For some time these programs have converged into three main fields, /6/, with different requirements from implemented mathematical models. These fields are process simulation, structure simulation, and material simulation.

Simufact Welding includes process and structure simulation. This software uses a mathematical heat model that can simulate any arc process through adequate geometry of heat source /6/. Heat source modelling is the most difficult challenge in simulating the heat distribution field which directly influences the quality of the welded joint. The first attempt in solving this problem was an analytical model of point heat source /7/. After this model, the concept was broadened to surface sources such as Gaussian heat sources. Improvements in computing power and the development of numerical methods have led to the development of volumetric sources such as conical heat sources, and the currently most used is the double ellipsoid source, developed by Goldak /8/. Goldak's heat model is used in Simufact Welding software, /9/, as a heat source for arc processes, as well as in other applications, /10, 11/.

For the purpose of this simulation, the gas metal arc welding (GMAW or MIG) process is chosen as it is the most common and fastest welding process. Numerical simulation of lap joint for alloy AA6060-T4 is selected for the study. This alloy is chosen because it is commonly used in many applications, from piping, architecture, automobile industry, pneumatic installations, and many more, because of its relatively good weldability.

MATHEMATICAL MODEL

A moving heat source is a phenomenon in heat transfer that is applicable in many engineering tasks, especially in the field of welding. From theoretical solutions of this problem, it is possible to determine the temperature distribution and cooling rate, allowing engineers to better understand the consequences of heat input and performance of the final product. Practical applications of these solutions in welding are reflected in the determination of microstructure, joint strength, residual stresses, cold cracking, size of the heat-affected zone (HAZ), and deformation /8/.

Since the temperature of the material during welding changes, we have a case of a three-dimensional non-stationary heat transfer problem. For plate welding with heat generation, this problem can be described by the Fourier heat equation:

$$\frac{\partial T}{\partial t}=\alpha\nabla^2 T+\dot{Q}\,, \tag{1}$$

$$\frac{\partial}{\partial x'}\left(\frac{k}{\rho c}\frac{\partial T}{\partial x'}\right)+\frac{\partial}{\partial y'}\left(\frac{k}{\rho c}\frac{\partial T}{\partial y'}\right)+\frac{\partial}{\partial z'}\left(\frac{k}{\rho c}\frac{\partial T}{\partial z'}\right)=\frac{\partial T}{\partial t}+\dot{Q}\,, \tag{2}$$

where: T-temperature; k-coefficient of thermal conductivity; ρ-material density; c-specific heat of testpiece; $\alpha = k/\rho c$ is thermal diffusivity; x'-direction along welded joint; y'-direction along the cross-section; z'-direction along material thickness; $\dot{Q}$ -heat from source; and t is time.

We can conclude that the dimensions of the heat source are far smaller than the testpiece and consider it as a point heat source. Except at the beginning and end of the welding process, the temperature distribution in the testpiece is stationary, as observed from the moving coordinate system located in the heat source and moves along with it. Under such conditions, the time variable in the process disappears and the process is reduced to quasi-stationary, allowing us to adopt the following substitution and observe the problem from a moving coordinate system, /12/:

$$x=x'-vt,\quad y=y',\quad z=z'\,, \tag{3}$$

where: v is speed of the moving coordinate system and thus speed of moving heat source. After this, we transform time dependence into spatial:

$$\frac{\partial T}{\partial t}=\frac{\partial T dx}{\partial x dt}=-v\frac{\partial T}{\partial x}\,. \tag{4}$$

By adopting new variables, the initial equation is transformed into, /9/:

$$\frac{k}{\rho c}\left(\frac{\partial^2 T}{\partial x^2}+\frac{\partial^2 T}{\partial y^2}+\frac{\partial^2 T}{\partial z^2}\right)+v\frac{\partial T}{\partial x}=\dot{Q}\,. \tag{5}$$

The heat coming from the heat source is obtained on the basis of Joule's law:

$$\dot{Q}=UI\eta\,, \tag{6}$$

where: U is voltage; I is electrical current; and η is the efficiency of the electric arc.

Goldak's heat source model, a double ellipsoid, most truly represents the heat source in arc welding. This geometry is made up of quadrants of two different ellipsoids. Calculations have shown that the temperature gradient below the heat source is not as steep as the gradient on the accompanying side, which is why it is described with two ellipsoids of different parameters, /7/:

$$q_f=q(x,y,z)=\frac{6\sqrt{3}f_f\dot{Q}}{abc_f\pi\sqrt{\pi}}e^{-3x^2/a_f^2}e^{-3y^2/b^2}e^{-3z^2/d^2}\,, \tag{7}$$

$$q_r=q(x,y,z)=\frac{6\sqrt{3}f_r\dot{Q}}{abc_r\pi\sqrt{\pi}}e^{-3x^2/a_r^2}e^{-3y^2/b^2}e^{-3z^2/d^2}\,, \tag{8}$$

In Eqs. (7) and (8), f_f and f_r are fractions of heat flux in the front and rear quadrant, where $f_f + f_r = 2$; a_f, a_r, b, d are geometric parameters that define the size and shape of ellipsoids and thus heat distribution. Geometric parameters are independent and can have different values, for example for heterogeneous materials, Goldak's heat source would consist of four octants, with different values of geometric parameters, /8/.

NUMERICAL SIMULATION

The numerical simulation here is performed to analyse effects of different welding sequences on residual stresses occurring in the material, as well as distortions of welded parts which are a direct consequence of residual stresses.

Two aluminium plates made of AA6060-T4 alloy are used as welded testpieces in this simulation. The thickness of individual plates is t = 5 mm, and their width and length are a = 150 mm and b = 500 mm. Welds of the lap joint are performed consecutively.

SIMULATION SETUP

Simufact Welding software, /9/, used in the simulation does not have the capability to form a CAD (Computer-Aided Design) model nor can generate the finite element mesh, so these tasks had to be done using other software. This software can work only with meshes in '.bdf' (bulk data file), used by only a few programs. The recommended mesh for this software is hexahedral /9/, and to obtain the best simulation results, the created mesh is also conformal.

Minimum overlapping in the joint is five times the thickness of thinner material in order to prevent joint rotation phenomenon /13/. In this simulation, an overlap of 30 mm is adopted. The created geometry is divided into three sections for meshing, Fig. 1. The first segment width is 50 mm with the finest mesh size of 2.5 mm elements, since this is the area of the weld path and the heat affected zone HAZ, and thus an area for observation. The second segment has a width of 2.5 mm and represents a transition zone between fine and coarse mesh, which allows for conformal mesh creation. The third zone width is 97.5 mm and it is the farthest from the joint with adopted mesh size of 7.5 mm. The mesh is created by first making surface meshes of appropriate densities and then propagating it through the volume by 1.25 mm steps. The basic simulation configuration parameters are given in Table 1.

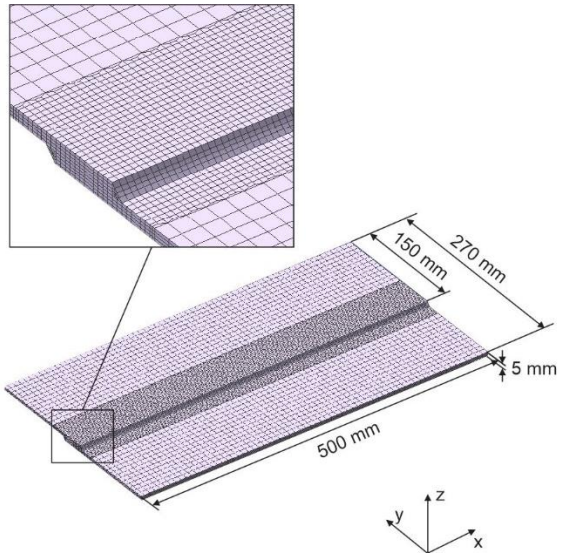

Figure 1. Testpieces with displayed mesh.

Table 1. Basic simulation parameters.

Process type	Arc welding
Ambient temperature	20°C
Gravity	9.80665 m/s^2
Gravity direction	*z*: -1
Components	2
Bearings	2
Clampings	2
Robotic arm	1
Component material	AA6060-T4
Filler material	AA5356
Convective heat transfer coefficient – h	20 W/m^{2}K
Contact heat transfer coefficient – a	automatic
Emission coefficient – ε	0.09

Both components are of AA6060-T4 material, and as a filler material, the alloy AA5356 is selected /14/. Two clamps of circular cross-section diameter 40 mm are used and are located at the upper side for clamping the testpieces with a force of 400 N. At the bottom are two bearings of the same size as the clamps, and are located directly below them, Fig. 2. Convective heat transfer coefficient is taken for a case of free convection in air h = 20 W/m^{2}K, /15/. Since the contact heat transfer coefficient depends on pressure between surfaces in contact, among other factors it is automatically calculated by the software, being an available option. For the emissivity coefficient, the value for sheet aluminium is taken as ε = 0.09, /16/.

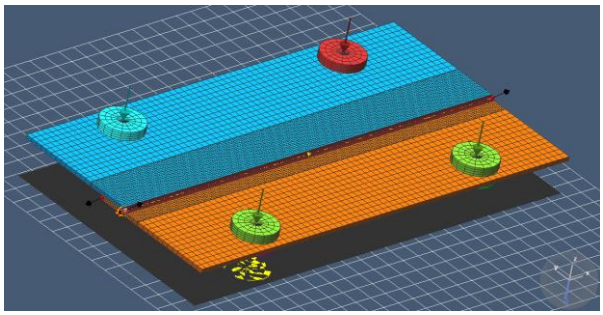

Figure 2. Testpeices with mechanical constraints.

Clampings have a possibility to be removed at a specific moment. Ideally, this would be done only when the temperature of all welded components drops to ambient temperature. In practice, this is unacceptable since it greatly affects the productivity of robotic welding arms. Therefore in this simulation, it is done 170 seconds since the start of the process as the temperature of welded components for all sequences drops below 90 °C.

WELDING PARAMETERS

The selection of welding parameters is taken for GMAW process of the fillet weld of aluminium $t \approx 5$ mm thickness, with AA5356 wire of 1.2 mm diameter. The position of welding is horizontal, and welding is executed in a single pass. For these settings, values for voltage, current, and welding speed are given in Table 2. The average efficiency of the GMAW process is η = 0.85, /17/.

Table 2. Welding parameters /14/.

Mode	Transient - indirect power
Welding voltage (U)	22.6 V
Welding current (I)	187 A
Efficiency (η)	0.85
Welding speed (v)	1050 mm/min

Based on these parameters, we can calculate the amount of heat introduced by the length of the seam according to:

$$E_s = \frac{UI}{v}\eta\,, \tag{9}$$

by using values from Table 2, one gets 205.273 J/mm.

Weld profile of the simulation is fillet, defined by four geometric values and mesh quality according to Fig. 3. Based on these values, a surface mesh of weld profile is generated.

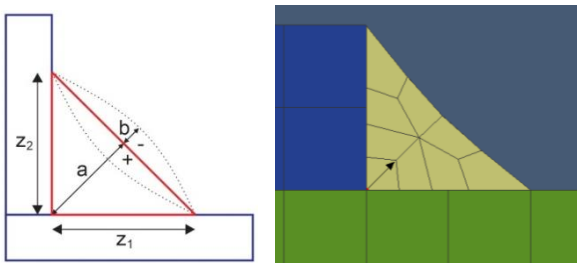

Figure 3. Weld profile input values (left), and simulation weld profile (right).

By inputting the following values: z_1 = 5 mm, z_2 = 5 mm, and b = 0.3 mm, mesh quality - medium, the software automatically calculates throat size a = 3.53 mm. As a heat source, Goldak's double ellipsoid is adopted as the best approach in modelling arc processes, Fig. 4.

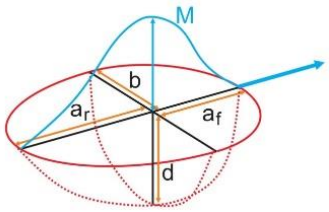

Figure 4. Heat source geometry.

Width b represents half of the width of the real weld pool. This as well as the value of depth d can be experimentally identified by micrographic analysis of melt pool and all other geometry values can be determined based on these two.

If micrographic results are not available, like in this simulation, they can be determined based on fillet throat size by following the expressions, /9/:

$$d = a + 2\ldots5 \text{ mm} = 7.53 \text{ mm}, \quad (10)$$

$$b = a + 1\ldots2 \text{ mm} = 5.03 \text{ mm}, \quad (11)$$

$$a_f = 0.6(a + 1.5 \text{ mm}) = 3.02 \text{ mm}, \quad (12)$$

$$a_r = 2.2(a + 1.5 \text{ mm}) = 11.07 \text{ mm}, \quad (13)$$

The Gaussian parameter defines the width of Gaussian distribution, in other words energy per area. For a very high value of the factor, we get a very narrow Gaussian curve and the opposite. The adopted value for this simulation is M = 3, /9/. The blue arrow indicates the direction of movement of the heat source, Fig. 4.

WELDING SEQUENCES

In the arc welding process, metal is locally heated and the heated zone is restrained by the surrounding cold metal. This generates stresses higher than material yield stress and causes permanent distortion. The level of distortion caused by the process is affected by multiple factors: parent material properties, restraint, joint design, edge preparation, and the welding procedure itself, /18/.

When it comes to welding procedures, general rules in reducing distortion are using as little weld metal as needed in as fewest passes as possible, but also to balance shrinkage forces around the neutral axis of the part, and use intermittent welds instead of continuous, /3/.

Another very important distortion control technique is the manipulation of welding sequence which is the objective of this paper. Three approaches are tested, first is the *back-step* in which welds are broken into short sections that are welded in the opposite direction of general weld progression. For example, if the weld is progressing from left to right, segment's beads are deposited from right to left. The second method is *skip-stop* welding. The direction of welding is the same as in the back-step method, except that segments are not made in a continuous sequence. For example, the first one is welded, the second one is skipped, then the third weld is applied, etc. The third strategy is welding from the joint centre towards the ends.

In Fig. 5, it can be seen that welds are divided into four segments whose order is varied in simulations. The red arrow shows a general progression of the weld.

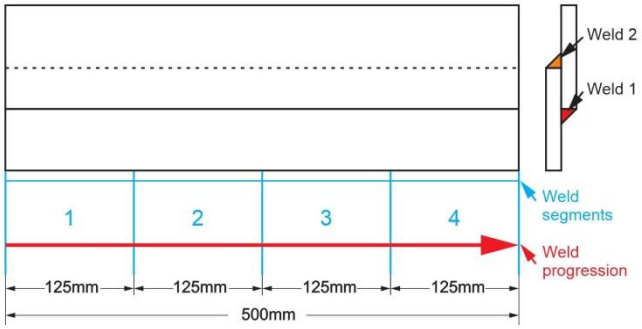

Figure 5. Weld segments.

A simulation plan with variations of welding sequences is given in Table 3. *Weld* 1 and *Weld* 2 are done consecutively. Four welding approaches are tested in this simulation. The first one is without change of welding segment order, the second one is *beck-step*, the third is *skip-stop* method, and the fourth is from joint centres toward the ends. These four approaches are tested for both welds in the same direction, and after that are repeated, but this time, the weld direction is opposite, in a way that the direction of Weld 2 is opposite to the weld progression direction. From this, we see that the simulation plan has eight points. For simplicity of segment direction notation, the sign '–' before segment number marks the direction opposite to weld progression, and sign '+' before segment number, the same direction as weld progression.

Table 3. Simulation sequences.

Sequence nr.	Sequence strategy	Sequence order of weld 1	Sequence order of weld 2
Sequence 1	None	+1,+2,+3,+4	+1,+2,+3,+4
Sequence 2	None	+1,+2,+3,+4	-4,-3,-2,-1
Sequence 3	Back-step	-1,-2,-3,+4	-1,-2,-3,+4
Sequence 4	Back-step	-1,-2,-3,+4	+4,+3,+2,-1
Sequence 5	Skip-stop	-1,-3,+4,-2	-1,-3,+4,-2
Sequence 6	Skip-stop	-1,-3,+4,-2	+4,+2,-1,+3
Sequence 7	From centre	-2,+3,-1,+4	-2,+3,-1,+4
Sequence 8	From centre	-2,+3,-1,+4	+3,-2,+4,-1

It can be observed that the last segment is always welded towards the edge of the testpiece. This is done to prevent starting the arc on the edge, which in practice gives poor weld area.

RESULTS AND DISCUSSION

The simulation considers the period of 420 s from the beginning of the process. After this period, the temperature of welded testpieces for all sequences is less than 45 °C. Further monitoring of the process results only in a longer duration of the simulation, without changing the order of the results of the dependence of the degree of distortion from the welding sequences. The results show that the variation of the welding order has the greatest influence on the distortion in the *Z*-axis direction, which could be expected due to the orientation of the testpieces. The absolute values of these distortions are presented in Fig. 6.

We can observe that the best values are obtained in Sequence 8, where the two-direction method from the centre is used because we have the smallest absolute distortion (Fig. 6). If we compare these values with Sequence 1 which has the highest *Z*-axis distortion result of ≈ 45 % higher, we can see the positive effects of this approach. Distortion as a phenomenon in arc welding is a direct consequence of developed internal stresses in the material which are introduced by the sudden change in temperature from the electric arc, Fig. 7. Therefore, when testing the welding distortion, the most important parameters are the residual stresses and the peak temperatures that occur in the material (Figs. 8 and 9).

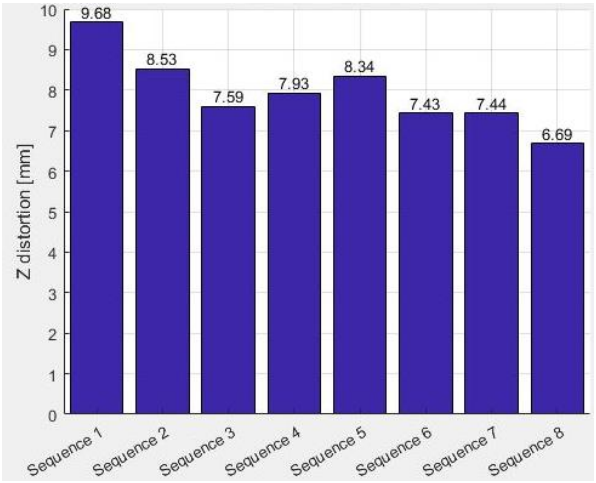

Figure 6. Absolute *Z*-axis distortion results.

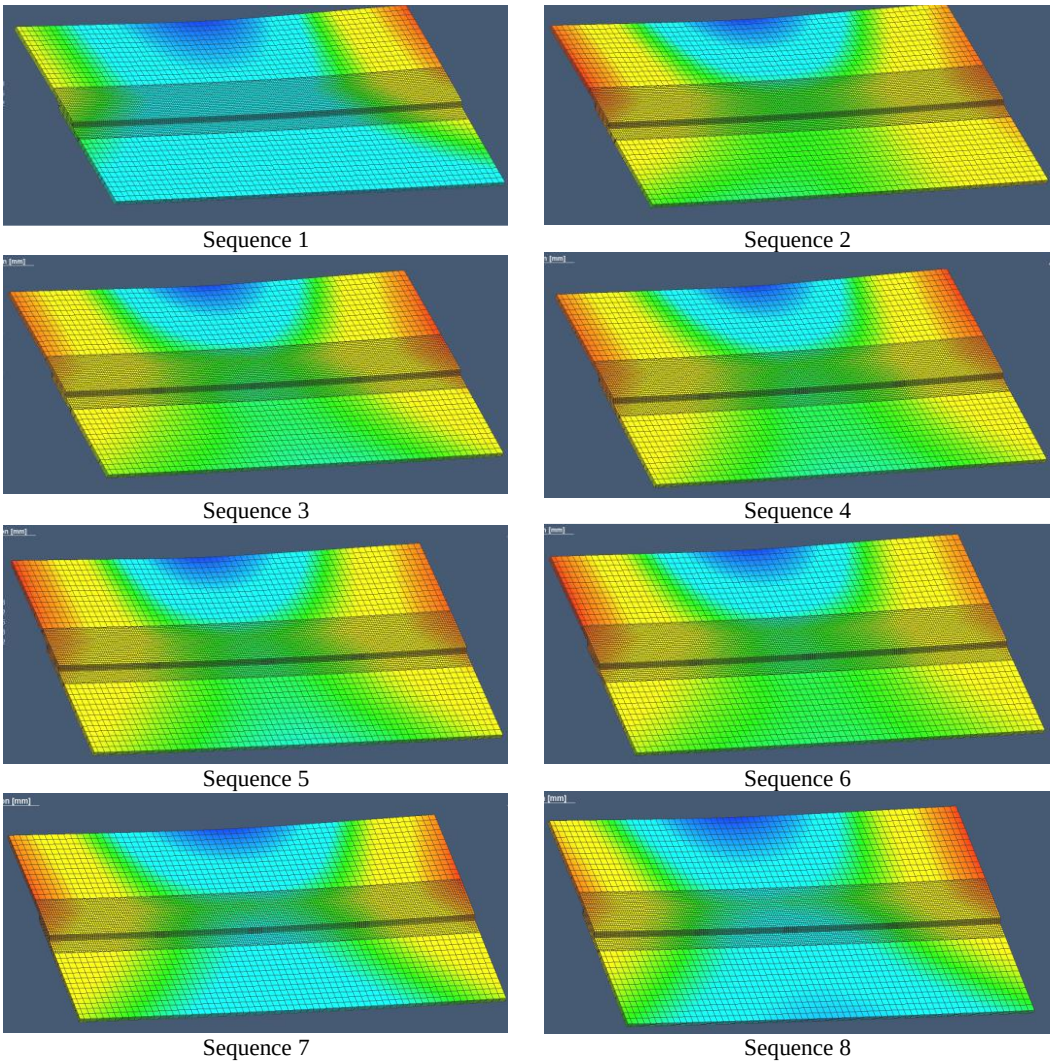

Figure 7. Distribution of distortion values on testpieces.

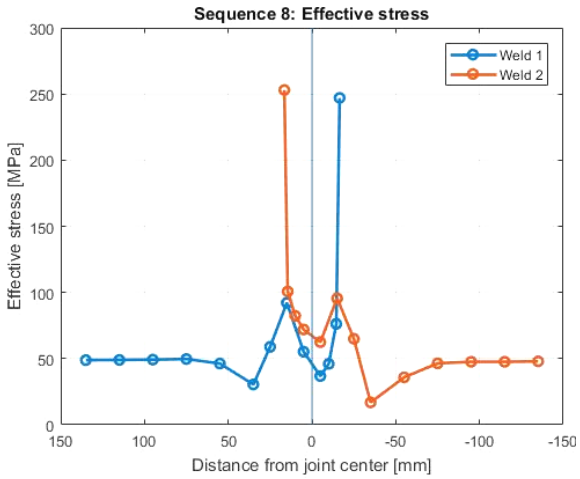

Figure 8. Residual stress distribution in a cross-section of welded testpieces (*YZ* plane), for Sequence 8.

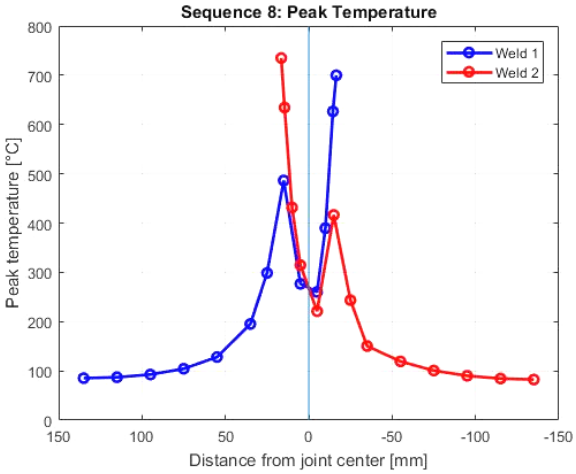

Figure 9. Peak temperature in cross-section of welded testpieces (*YZ* plane), for Sequence 8.

The electric arc for each segment, except for the first one in the process is started by overlapping the closest weld to the starting point of the segment by 15 mm. To avoid the influence of this additional heat input, a cross-section in the *YZ* plane isn't taken at the middle of the joint, but offset for 50 mm, at X = 300 mm. Results of peak temperature and residual stress for two extreme cases are compared, Figs. 10-13.

Figures 8-11 show the distribution of effective stress and peak temperature through the cross-section of the testpieces, with a value of 0 on the axis representing the centreline of the lap joint. We can see that the highest values of both parameters rest on the weld itself and in HAZ. Since the joint consists of two welds, in both samples, we have two HAZ's and two peaks. The second peak is smaller because the values are taken from the middle (seen along the *Y*-axis) of the testpieces and insulated with more material compared to the first, which is ending directly in the welded joint.

As the distance from the weld increases, the maximum temperature value gradually decreases (Fig. 9). For the effective stress value, we can notice a sudden drop outside the HAZ, and the stress increases again (Fig. 10).

Comparing these values for the sequence with the smallest and largest distortion, we cannot notice significant differences in cross-section.

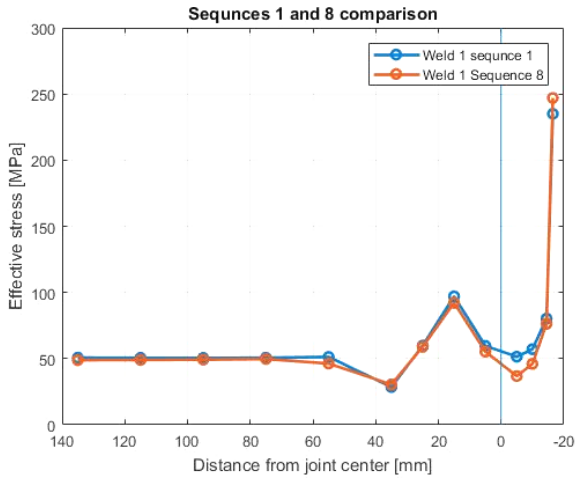

Figure 10. Comparison of residual stresses at Sequence 1 (largest distortion) and Sequence 8 (smallest distortion) in *YZ* plane of Weld 1.

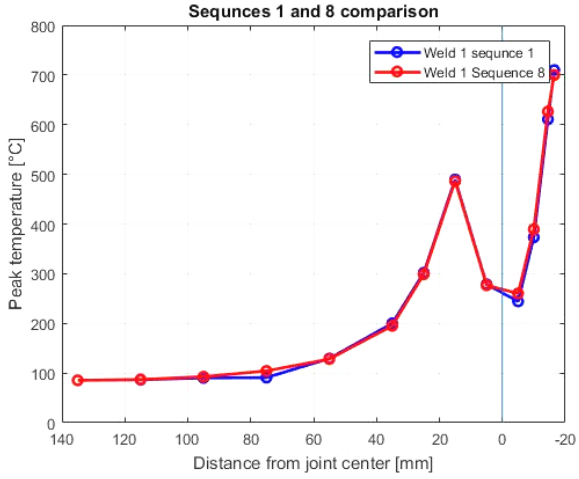

Figure 11. Comparison of peak temperature at Sequence 1 and Sequence 8 in the *YZ* plane of Weld 1.

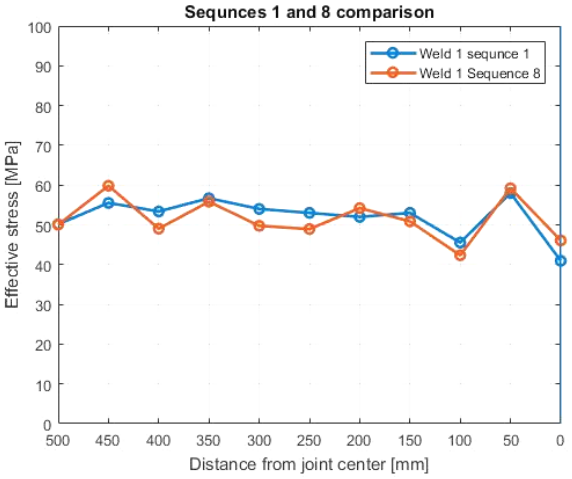

Figure 12. Comparison of residual stress values at Sequence 1 and Sequence 8 in the longitudinal section (*XZ* plane) at Weld 1.

If we compare the results in the longitudinal section for the two extreme cases (Figs. 12 and 13), we can see the inequality of results. We see that the differences in the results are significantly smaller for Sequence 8, where we have more stable values. This can be seen especially in

temperature variations, e.g., the maximum temperature of Sequence 1 is +305 °C, and the minimum is +219 °C. For Sequence 8 these temperatures are +268.4 and +235°C.

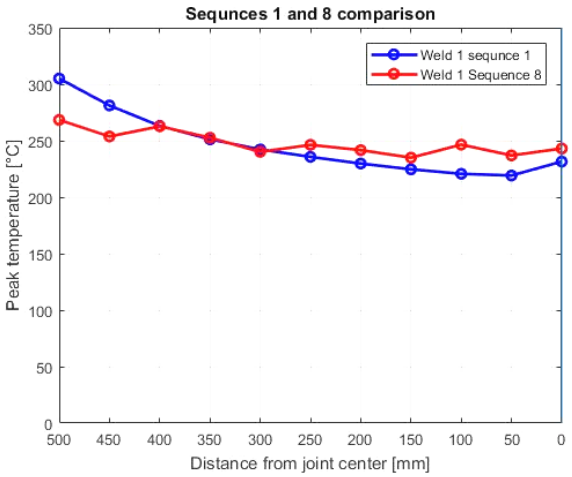

Figure 13. Comparison of peak temperature at Sequence 1 and Sequence 8 in the longitudinal section of Weld 1.

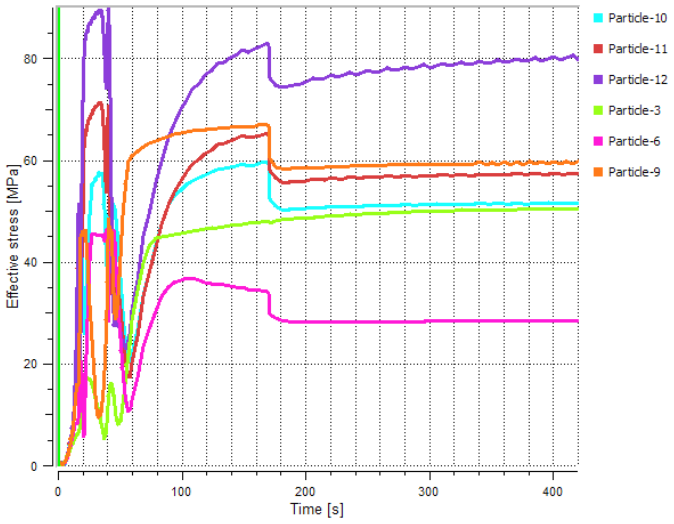

Figure 14. Residual stresses at selected cross-section points as a function of time.

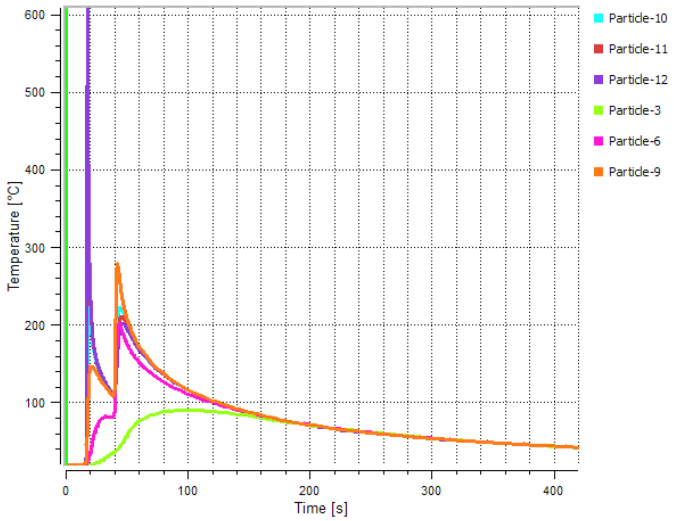

Figure 15. Temperature at selected cross-section points as a function of time.

Figures 14 and 15 show the temperature and residual stresses as a function of time at 6 points in the cross-section, starting from Particle 3 which is farthest from the welded joint to Particle 12 located next to the weld metal. We can notice large variations of all values during the first 60 seconds of the welding process. This is followed by a gradual decrease in temperature in all analysed points, and in contrast, an increase of residual stresses. When it comes to stresses, there is a sudden drop in 170 seconds, because the release of mechanical boundary conditions, i.e. the clamps, takes place, and so the material is allowed to deform freely.

CONCLUSION

Distortion of the welded structures as the consequence of heat input and developed residual stresses is an easily observable parameter of welded joint quality. In this paper, a simulation of the lap joint is conducted based on the experimental plan in which different strategies of welding sequences are executed. Results of the two extreme cases of the experiment are compared. The largest difference in the results occurs in the longitudinal section. From this result, we can conclude that the main cause of increased distortion is the unevenness in the levels of maximum temperature and residual stresses, which leads to increased values of distortion. For the cross-section, major differences in values cannot be observed.

It is not possible to eliminate unwanted distortions in welding procedures. This phenomenon becomes more pronounced with increase in weld length. The conducted research illustrates that by implementing an adequate welding sequence strategy, distortions can be lowered as much as 30 %.

REFERENCES

1. Mackerle, J. (2003), *Finite element analysis and simulation of polymers-an addendum: a bibliography (1996-2002)*, Model. Simul. Mater. Sci. Eng. 11(2): 195-231. doi: 10.1088/0965-0393/11/2/307
2. Bonhart, E.R., Welding: Principles and Practices, 5th Ed., McGraw-Hill Education, 2017.
3. Bajić, D., Postupci zavarivanja (*Welding Procedures*), University of Montenegro, Department of Mechanical Engineering, 2014.
4. Khoshroyan, A., Darvazi, A.R. (2020), *Effects of welding parameters and welding sequence on residual stress and distortion in Al6061-T6 aluminum alloy for T-shaped welded joint*, Trans. Nonferrous Met. Soc. China, 30(1): 76-89. doi: 10.1016/S1003-6326(19)65181-2
5. Romero-Hdz, J., Toledo-Ramirez, G., Saha, B. (2017), *Deformation and residual stress based multi-objective genetic algorithm for welding sequence optimization*, Res. Comput. Sci. 132(1): 155-179. doi: 10.13053/rcs-132-1-12
6. Simulating Welding with Simufact Welding - Simufact Engineering GMBH. https://www.simufact.com/simufactwelding-welding-simulation.html (last accessed Sep. 18, 2021)
7. Farias, R.M., Teixeira, P.R.F., Vilarinho, L.O. (2021), *An efficient computational approach for heat source optimization in numerical simulations of arc welding processes*, J Constr. Steel Res. 176: 106382. doi: 10.1016/j.jcsr.2020.106382
8. Goldak, J., Chakravarti, A., Bibby, M. (1984), *A new finite element model for welding heat sources*, Metall. Mater. Trans. B, 15(1): 299-305. doi: 10.1007/BF02667333

9. S.W. Simulation, Simufact Welding 6.0
10. Ivanović, I., Sedmak, A., Miloš, M., et al. (2011), *Numerical study of transient three-dimensional heat conduction problem with a moving heat source*, Thermal Sci. 15(1): 257-266. doi: 10.2298/TSCI1101257I
11. Veljić, D., Perović, M., Sedmak, A., et al. (2011), *Numerical simulation of the plunge stage in friction stir welding*, Struct. Integ. and Life, 11(2): 131-134.
12. Yeh, R.H., Liaw, S.P., Yu, H.B. (2003), *Thermal analysis of welding on aluminum plates*, J Marine Sci. Technol. 11(4): 213 -220.
13. Miller, D.K. (2001), *Designing welded lap joints*, Weld. Innov. XVIII(3): 6-8.
14. Lincoln Electric, 'Aluminium GMAW for Aluminium Guide,' pp. 1-69, 2016. www.lincolnelectric.com
15. Kosky, P., Balmer, R., Keat, W., Wise, G., Convection Heat Transfer Coefficient - An Overview, In: Exploring Engineering, 3rd Ed., 2013. doi: 10.1016/B978-0-12-415891-7.09998-2
16. Anon., 'Emissivity Coefficient Materials,' Engineering Tool Box, 2003. https://www.engineeringtoolbox.com/emissivity-coefficients-d_447.html (last accessed Sep. 18, 2021)
17. Pépe, N., Egerland, S., Colegrove, P.A., et al. (2011), *Measuring the process efficiency of controlled gas metal arc welding processes*, Sci. Technol. Weld. Join. 16(5): 412-417. doi: 10.1179/1362171810Y.0000000029
18. Kumar, H., Optimization of angular distortion of TIG welded joint of mild steel and stainless steel, Master Thesis, National Institute of Technology, Kurukshetra, Thānesar, Haryana, India, 2018, 56 p.